The Journal of Experimental Medicine

Early, transient depletion of plasmacytoid dendritic cells ameliorates autoimmunity in a lupus model

Sarah L. Rowland,[1] Jeffrey M. Riggs,[2] Susan Gilfillan,[1] Mattia Bugatti,[3] William Vermi,[1,3] Roland Kolbeck,[2] Emil R. Unanue,[1] Miguel A. Sanjuan,[2] and Marco Colonna[1]

[1]Department of Pathology and Immunology, Washington University School of Medicine, St. Louis, MO 63110
[2]Respiratory, Inflammation and Autoimmunity Research Department, MedImmune, Gaithersburg, MD 20878
[3]Department of Pathology, University of Brescia, 25123 Brescia, Italy

Plasmacytoid dendritic cells (pDCs) have long been implicated in the pathogenesis of lupus. However, this conclusion has been largely based on a correlative link between the copious production of IFN-α/β by pDCs and the IFN-α/β "signature" often seen in human lupus patients. The specific contribution of pDCs to disease in vivo has not been investigated in detail. For this reason, we generated a strain of BXSB lupus–prone mice in which pDCs can be selectively depleted in vivo. Early, transient ablation of pDCs before disease initiation resulted in reduced splenomegaly and lymphadenopathy, impaired expansion and activation of T and B cells, reduced antibodies against nuclear autoantigens and improved kidney pathology. Amelioration of pathology coincided with decreased transcription of IFN-α/β–induced genes in tissues. PDC depletion had an immediate impact on the activation of immune cells, and importantly, the beneficial effects on pathology were sustained even though pDCs later recovered, indicating an early pDC contribution to disease. Together, our findings demonstrate a critical function for pDCs during the IFN-α/β–dependent initiation of autoimmune lupus and point to pDCs as an attractive therapeutic target for the treatment of SLE.

CORRESPONDENCE
Marco Colonna:
mcolonna@pathology.wustl.edu

Abbreviations used: ABC, age-associated B cell; ANA, anti-nuclear autoantibody; cDC, conventional DC; DN, CD23⁻ CD21⁻ double negative B cell; DT, diphtheria toxin; DTR, diphtheria toxin receptor; IFNAR, IFN-αβ receptor; ISG, IFN-stimulated gene; MPO, myeloperoxidase; MZ, marginal zone B cell; pDC, plasmacytoid DC; SLE, systemic lupus erythematosus; T1, transitional-1 B cell.

Systemic lupus erythematosus (SLE) is a chronic multiorgan autoimmune inflammatory disease that affects many organs and causes multiple pathologies, including but not limited to glomerulonephritis, arthritis, and skin lesions. SLE is characterized by a loss of tolerance to endogenous nuclear antigens, resulting in the production of autoantibodies that bind nuclear components, such as chromatin, double-stranded (ds) DNA, and ribonucleoproteins (RNP; Fairhurst et al., 2006; Shlomchik, 2009; Theofilopoulos et al., 2010). However, many studies indicate that dysregulation of innate immunity, particularly secretion of IFN-α, contributes to pathogenesis of SLE (Banchereau and Pascual, 2006; Marshak-Rothstein and Rifkin, 2007; Gilliet et al., 2008; Guiducci et al., 2009; Santer et al., 2009; Theofilopoulos et al., 2010; Elkon and Santer, 2012). SLE activity and autoantibody levels are associated with a marked IFN-α signature in the blood and skin (Baechler et al., 2003; Bennett et al., 2003; Crow et al., 2003). Nonautoimmune patients treated with soluble IFN-α can develop a lupuslike syndrome and accumulation of autoantibodies (Båve et al., 2003; Santiago-Raber et al., 2003). Viral infections, UV-mediated skin injury, or other events leading to IFN-α production induce SLE flares. Mice strains that spontaneously develop a lupus-like disease have less severe disease when backcrossed to mice deficient for the receptor for IFN-α (IFNAR; Santiago-Raber et al., 2003) or when treated with an antibody that blocks the IFNAR (Baccala et al., 2012). IFNAR-deficient mice are resistant to induction of experimental lupus (Nacionales et al., 2007).

Plasmacytoid DCs (pDCs) are bone marrow–derived cells that specialize in the secretion of IFN-α/β in response to viral infections

(Gilliet et al., 2008). PDCs detect viral nucleic acids and their synthetic analogues through TLR7 and TLR9, which are located in specialized endosomes (Barbalat et al., 2010; Theofilopoulos et al., 2010). These receptors trigger a MyD88-dependent signaling pathway that leads to production of IFN-α/β, as well as IL-12, IL-6, and various other proinflammatory chemokines. Several studies have suggested that pDCs are also a major source of IFN-α in SLE. PDCs infiltrate the skin lesions of SLE patients (Farkas et al., 2001); they also secrete IFN-α after Fc-receptor–mediated endocytosis of autoantibody–nucleic acid immune complexes and delivery of nucleic acids to the TLR7- and TLR9-containing endosomes (Dzionek et al., 2001; Båve et al., 2003; Barrat et al., 2005; Means et al., 2005; Vollmer et al., 2005). pDCs also secrete IFN-α in responses to neutrophils that die after exposure to SLE-derived antiribonucleoprotein antibodies. Dead neutrophils release neutrophil extracellular traps (NETs), which contain endogenous DNA that enters pDC endocytic compartments after forming complexes with cationic proteins (Lande et al., 2007; Tian et al., 2007; Garcia-Romo et al., 2011).

Although these studies indicate that pDC secretion of IFN-α may contribute to the pathogenesis of SLE, the data linking pDCs to SLE are largely correlative and the specific role of pDCs in SLE pathogenesis has not been directly addressed. The study of pDCs in vivo has historically relied on the use of depleting monoclonal antibodies (Asselin-Paturel et al., 2001; Blasius et al., 2006). However, pDC-depleting mAbs are cross-reactive and eliminate many other cells in addition to pDC, yielding ambiguous phenotypes. To avoid these complications, we generated transgenic (tg) mice that express the diphtheria toxin receptor (DTR) under the control of the highly specific human pDC promoter, *CLEC4C* or *BDCA2,* in which administration of diphtheria toxin (DT) results in the selective systemic ablation of pDCs. More than 95% of pDCs are depleted within 24 h after initial DT treatment (Swiecki et al., 2010). Importantly, BDCA2-DTR tg mice tolerate repeated injections of DT with no detrimental effects, permitting long-term depletion of pDCs (Swiecki et al., 2010). To evaluate the impact of pDCs in the pathogenesis of SLE, we backcrossed the BDCA2-DTR transgene onto the autoimmune-prone BXSB background. BXSB is a recombinant inbred strain that recapitulates the proliferative glomerulonephritis observed in human SLE. BXSB mice develop anti-nuclear autoantibodies (ANA), including anti-dsDNA, -ssDNA, -RNP, and -ssRNA, as well as splenomegaly and lymphadenopathy. Disease susceptibility in BXSB is linked to several genetic loci, particularly the telomeric region of chromosome 1, which encodes Fcr2b, Ifi202, and SLAM/CD2 family members (Morel et al., 2001; Lauwerys and Wakeland, 2005; Fairhurst et al., 2006; Haywood et al., 2006; Theofilopoulos et al., 2010). Moreover, BXSB mice express the Y chromosome–linked autoimmune accelerator gene *Yaa.* The *Yaa* mutation arose from a translocation from the telomeric end of the X chromosome onto the Y chromosome, and contains the gene encoding TLR7 (Pisitkun et al., 2006; Subramanian et al., 2006). Thus, the *Yaa* mutation

results in duplication and increased expression of TLR7 in male mice, which causes accelerated autoimmunity (Deane et al., 2007; Fairhurst et al., 2008).

Our analysis of pDC depletion in BXSB.DTR mice indicates that pDCs are important for the initiation of lupus. We find reduced activation and expansion of immune cells, limited autoantibody production, and less severe glomerulonephritis when pDCs are depleted during the early stage of disease; this general alleviation of pathology coincides with decreased transcription of IFN-stimulated genes (ISGs) after pDC ablation. Our data indicate that the pathogenic effects of pDCs are particularly important during the early phase of disease, as a transient depletion was sufficient to ameliorate disease in BXSB.DTR mice. PDCs, therefore, represent an attractive therapeutic target for the treatment of SLE.

RESULTS
Specific depletion of pDCs in lupus–prone BXSB.DTR mice
To evaluate the contribution of pDCs to the pathogenesis of lupus, we serially backcrossed the BDCA2-DTR transgene to lupus-prone BXSB/MpJ mice, generating BXSBxBDCA2-DTR Tg mice (referred to throughout as BXSB.DTR mice). Lupus susceptibility loci on BXSB chromosome 1 were selected for until homozygous for BXSB alleles using 4 SSLP markers adjacent to known lupus susceptibility loci: D1Mit 231 (12cM), D1Mit156 (32.8 cM), D1Mit387 (62 cM), and D1Mit356 (95.8 cM; Haywood et al., 2006), and the BXSBY chromosome was maintained during breeding. Our breeding scheme produced BXSB littermates that expressed the DTR (BXSB.DTR+) and those that did not (BXSB.DTR−). BXSB.DTR− mice served as lupus control animals that did not respond to DT treatment and remained pDC sufficient for the duration of the experiments. Importantly, DT-treated BXSB.DTR− mice also served as controls for any potential toxicity related to the DT treatments. The results obtained from all PDC-sufficient cohorts (BXSB.DTR− mice treated with either DT or PBS and BXSB.DTR+ mice treated with PBS) were consistent among the groups with no significant differences between the two treatments. Thus, as for BDCA2-DTR Tg mice, pDC depletion after repeated injections of DT was effective and well tolerated in autoimmune BXSB.DTR mice (Fig. 1 A and not depicted).

Transient pDC depletion results in persistently impaired T cell activation in BXSB.DTR mice
We sought to examine the effect of early pDC ablation on the progression of disease. Male BXSB.DTR+ mice were transiently depleted of pDCs before the onset of clinical symptoms by twice-weekly injections of DT from 8 to 11 wk of age. PDC depletion was verified in a cohort of 11-wk-old mice after the final DT treatment. More than 95% ablation was achieved in the spleen, even after repeated injections of DT (Fig. 1 A). We found no effect on the pDC compartment when littermate control animals that did not express the DTR transgene (BXSB.DTR−) were treated with DT (Fig. 1 A). A cohort of control BXSB.DTR− and BXSB.DTR+ animals
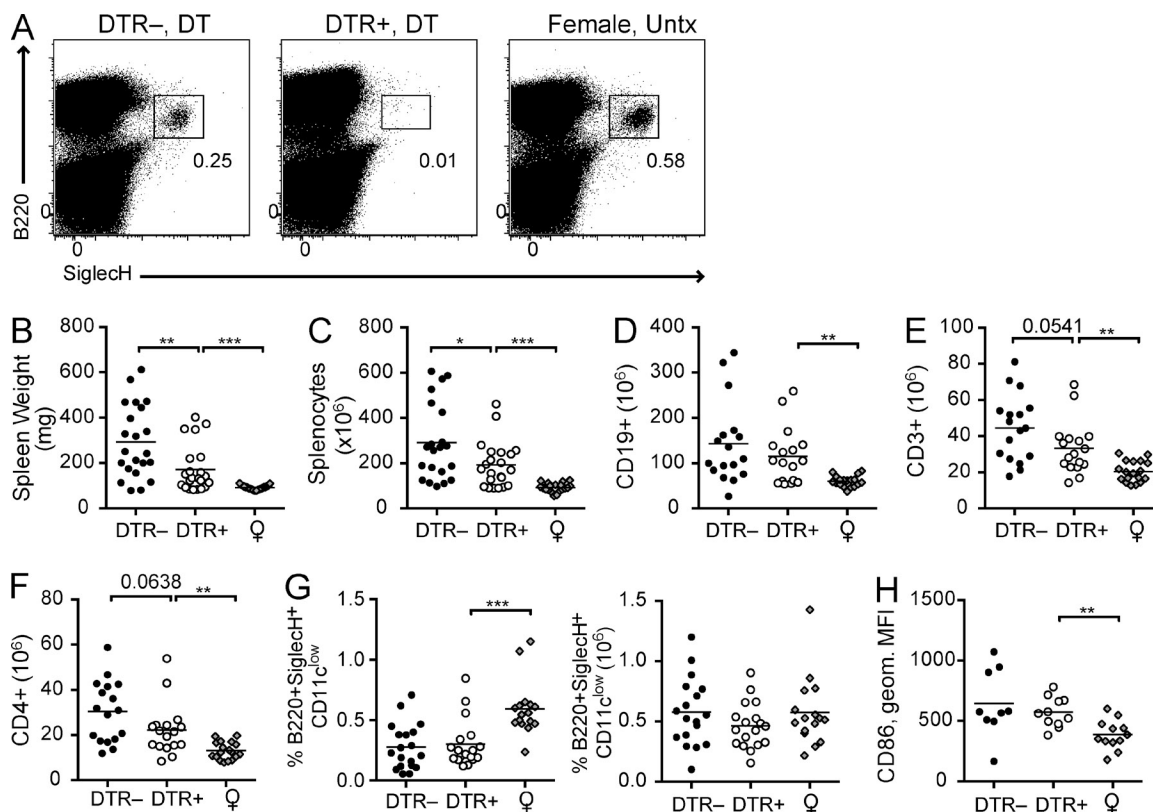
Figure 1. Reduced lymphoid organ hyperplasia in pDC–depleted BXSB.DTR mice. (A) Representative flow cytometric analysis of B220⁺SiglecH⁺ pDCs in spleen of 11-wk-old BXSB.DTR male littermates that were treated with DT as indicated. Female littermates were untreated (Untx). Spleen weight (B) and absolute spleen cell number (C) were determined in indicated mice. Number of CD19⁺ splenocytes (D), CD3⁺ splenocytes (E), and CD4⁺ splenic T cells (F) was determined by flow cytometry. (G) Frequency and absolute cell number of splenic pDCs and CD86 expression on splenic pDCs (H) was assessed by flow cytometry and CD86 expression is represented as geometric MFI. In B–H, male DTR⁺ and DTR⁻ mice were treated with DT and analyzed at 19 wk of age. Untreated, healthy female littermates are shown. Data points indicate individual mice grouped from 10–11 experiments. Bar indicates arithmetic mean. *, P < 0.5; **, P < 0.01; ***, P < 0.001. Absence of * indicates nonsignificant differences.

was treated concurrently with PBS (pDC-sufficient mice; not depicted). Depletion of pDCs was terminated when mice reached 11 wk of age and disease parameters were evaluated in 19-wk-old BXSB.DTR mice. After early pDC depletion, male BXSB.DTR mice had less marked splenomegaly and lymphadenopathy relative to male littermates that were pDC sufficient, and organ sizes were comparable to age-matched healthy female littermates (Fig. 1, B and C; and not depicted). The reduced cellularity was attributed primarily to a smaller number of T cells and, to a more variable extent, fewer B cells in the spleens of these mice. In particular, fewer CD4⁺ T cells were present after early pDC depletion (Fig. 1, D–F). We did not find a significant difference in the number of CD8⁺ T cells in pDC-depleted mice relative to male littermate controls (not depicted). However, parental male BXSB mice have been reported to have a diminished frequency of CD8⁺ T cells in comparison with age-matched female mice (Chu et al., 1994). Thus, although the overall number of CD8⁺ T cells is the same, this represents an increased frequency of CD8⁺ T cells in pDC-depleted mice relative to pDC-sufficient BXSB.DTR male mice and could be attributed to a rescue of the CD8⁺ T cell

population after pDC ablation. Importantly, pDC populations were equal in 19-wk-old BXSB.DTR male mice, irrespective of prior transient pDC depletion (Fig. 1 G). Moreover, pDCs in BXSB.DTR mice showed equivalent expression of CD86 and MHC II regardless of earlier depletion (Fig. 1 H and not depicted), suggesting that a comparable level of activation was achieved by the recovered pDC population. This pDC activation is likely caused by the duplication of TLR7 in BXSB.DTR male mice, as pDCs from female BXSB.DTR mice displayed lower levels of CD86 expression (Fig. 1 H).

We also observed fewer activated CD4⁺ and CD8⁺ T cells in pDC-depleted BXSB.DTR mice relative to pDC-sufficient male littermates (Fig. 2 and not depicted). The population of cells identified as CD44^high^CD62L^low/−^ was reduced in both T cell subsets (Fig. 2, A and B). The reduced frequency of activated CD44⁺ T cells correlated with an increase in the population of CD44⁻CD62L⁺ naive T cells (Fig. 2, A and C). In mice depleted of pDCs we also found fewer CD69⁺ CD8⁺ T cells (Fig. 2 D). No differences in the frequency of regulatory T cells was detected at this time, and we did not observe any changes in the frequency or activation state of CD11c⁺
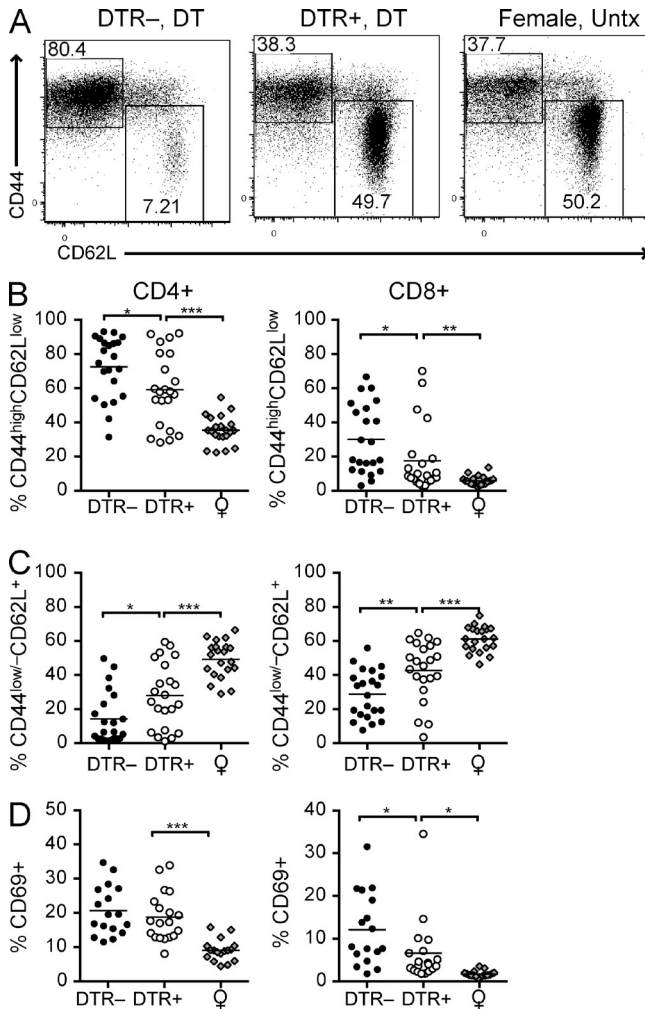
Figure 2. Transient pDC ablation impairs expansion and activation of T cells in BXSB.DTR mice. Male DTR⁺ and DTR⁻ mice were treated with DT and analyzed at 19 wk of age. Untreated, healthy female littermates are shown. (A) Representative flow cytometric analysis of CD44 and CD62L expression on CD4⁺CD3⁺ splenocytes in the indicated groups of mice. Frequency of CD44^high^CD62L^low^ (B), CD44^low/-^CD62L⁺ (C), and CD69⁺ CD4⁺ and CD69⁺CD8⁺ (D) T cells in spleen of the indicated mice were determined by flow cytometry. Data points indicate individual mice grouped from 10–11 experiments. Bar indicates arithmetic mean. *, P < 0.5; **, P < 0.01; ***, P < 0.001. Absence of * indicates nonsignificant differences.

or CD11b⁺ DC populations in the spleen, based on the level of MHC II and CD86 expression (unpublished data). We conclude that early transient pDC depletion persistently reduces T cell activation in BXSB.DTR mice.

Transient pDC depletion limits aberrant B cell development and generation of antinuclear autoantibodies in BXSB.DTR mice

It has been shown that male BXSB mice show features of abnormal B cell development (Amano et al., 2003). One prominent feature is the loss of the marginal zone (MZ) B cell population.

As reported for the BXSB/MpJ parental strain, pDC-sufficient BXSB.DTR control mice lost the CD23⁻CD21^high^ MZ B cell compartment by 19 wk of age. However, this compartment was restored when pDCs were depleted early during disease (Fig. 3, A and B).

Another abnormal B cell feature of the BXSB/MpJ parental strain, and several other autoimmune strains, is the presence of an unusual population of age-associated B cells (ABCs), which is also present in the peripheral blood of some autoimmune women (Rubtsov et al., 2011) and tends to accumulate in elderly normal female mice (Hao et al., 2011; Rubtsov et al., 2011). ABCs reside within the CD23⁻CD21⁻ double-negative (DN) B cell population, which also includes transitional-1 (T1) B cells. Although T1 B cells express AA4.1, ABCs are negative for AA4.1 and express CD11c and CD11b (Hao et al., 2011; Rubtsov et al., 2011). Early pDC depletion in BXSB.DTR male mice resulted in a reduction in the CD19⁺CD23⁻CD21⁻ DN spleen B cell population. Within the DN population, we observed a trend toward a decrease in the frequency of DN cells with the ABC phenotype (AA4.1⁻) and an increase in the frequency of DN cells exhibiting a T1 phenotype (AA4.1⁺), suggesting that pDCs contribute to the accumulation or expansion of ABCs (Fig. 3, A and C). Cells within the AA4.1⁻ population expressed CD11c, consistent with their identification as ABCs (Hao et al., 2011; Rubtsov et al., 2011; and unpublished data). Remarkably, a subset of pDC-sufficient male BXSB.DTR mice developed a noticeable population of DN cells in the lymph nodes that were never observed in healthy animals (Fig. 3 D and not depicted). Healthy female controls and male BXSB.DTR mice that were depleted of pDCs did not harbor this population within the lymph nodes, again corroborating that pDCs may promote the aberrant expansion of ABCs in lymph nodes during lupus.

We observed subtle effects on the other B cell compartments after pDC depletion. There was little change in the frequency of CD23^high^CD21^low^ transitional 2 (T2)/follicular (Fo) B cells in the spleen. However, although not significant, the absolute number of T2/Fo B cells tended to be slightly lower in pDC-depleted mice (unpublished data). The population of CD19^low/-^B220^low/-^CD138⁺ plasma cells remained relatively uniform among the mice (unpublished data). Despite little change in the frequencies of antibody-secreting cells, early pDC depletion resulted in reduced serum Ig relative to pDC-sufficient control animals. Circulating levels of IgG were reduced in the serum of pDC-depleted BXSB.DTR mice (Fig. 4 A). The overall prevalence of antinuclear autoantibodies (ANAs) was also reduced in DT treated BXSB.DTR⁺ mice relative to littermate control animals with an intact pDC compartment (Fig. 4 B). The decrease in serum immunoglobulin titers was not attributable to a single IgG isotype. Rather, IgM and all IgG subclasses were reduced in animals that were previously depleted of pDCs (Fig. 4, C and D). To determine which self-antigens were recognized, we performed a qualitative analysis to screen for autoantibody reactivity by autoantigen array. We
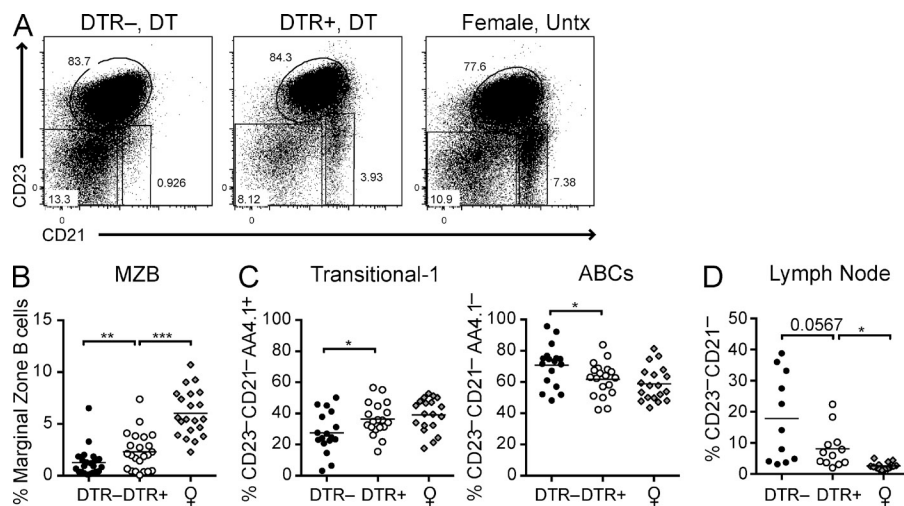
Figure 3. Transient pDC depletion reconstitutes MZ B cells and inhibits the development of ABCs. Male DTR+ and DTR− mice were treated with DT and analyzed at 19 wk of age. Untreated, healthy female littermates are shown. (A) Representative FACS analysis of CD23 and CD21 expression on CD19+ splenocytes. Frequencies of CD23−CD21^{high} MZ B cells (B) and CD23−CD21−AA4.1+ transitional-1 B cells and CD23−CD21−AA4.1− ABCs (C) in spleen of indicated mice were determined by flow cytometry. Frequencies of CD23−CD21−CD19+ cells in lymph node (D) of indicated mice were determined by flow cytometry. Data points indicate individual mice grouped from 10–11 experiments. Bar indicates arithmetic mean. *, $P < 0.5$; **, $P < 0.01$; ***, $P < 0.001$. Absence of * indicates nonsignificant differences.

observed a trend toward reduced antibody recognition of many lupus-associated antigens, including ssDNA, dsDNA, chromatin, and histones (Fig. 4, E and F), with recognition of Histone H2B the most reduced. However, not all lupus-associated antigens evaluated were significantly reduced at 19 wk of age after early pDC depletion. We found little difference in the prevalence of La/SSB–, sm/RNP–, or U1-snRNP–specific autoantibodies at this time (Fig. 4, E and F). It is important to note that data obtained from the autoantigen arrays are not quantitative, but rather indicate the specificity of antibodies present in the serum and relative autoantigen binding among lupusprone mice. Overall, these data demonstrate that transient pDC depletion limits aberrant B cell development and autoantibody production.

Suppression of glomerulonephritis in pDC–depleted BXSB.DTR mice

Male BXSB mice develop proliferative glomerulonephritis and immune complex deposition in the kidney as disease progresses. Consistent with this, BXSB.DTR lupus control mice had high proteinuria and developed severe renal pathology (Fig. 5, A and B). Glomerular hypercellularity, as well as increased mesangial matrix formation and thickening of glomerular membranes were evident in kidneys from pDC-sufficient control groups (Fig. 5, C and D). In contrast, BXSB.DTR mice subjected to early pDC ablation had less proteinuria and kidneys showed markedly less severe glomerular lesions, with limited cellular infiltrates and minimal matrix expansion or glomerular membrane thickening (Fig. 5, A–D). Moreover, IgG/C3 deposition in kidneys of BXSB.DTR mice was significantly reduced in mice that were depleted of pDCs (Fig. 5, E and F). CD3+ T cells and CD11b+ myeloid cells were abundant in the kidney infiltrating leukocytes of pDC-sufficient mice but were significantly reduced after pDC ablation (Fig. 5, G–J). Gr1+ cells were seen in some control BXSB.DTR littermates, but not found in any pDC-depleted animals (unpublished data). PDCs were not detected in any of the kidneys,

regardless of prior pDC depletion (unpublished data). We conclude that transient pDC depletion ameliorates end-point kidney pathology.

Reduced IFN–α/β gene signature in BXSB.DTR kidneys after transient pDC depletion

IFN–α/β–inducible genes are associated with the severity and progression of lupus (Baechler et al., 2003; Bennett et al., 2003; Crow et al., 2003). We observed reduced local expression of several IFN–α/β target genes, including *mx1, oas3, irf7,* and *ifit1,* in kidney from pDC-depleted animals in comparison to kidney from pDC-sufficient mice (Fig. 6). In contrast, we found that the expression of IFN–α/β gene targets in blood of 19-wk-old BXSB.DTR mice were unaffected by early pDC depletion (unpublished data). Together, these findings suggest that early pDC ablation can lead to sustained reduction of local tissue IFN–α/β, inhibiting the initiation of the pathological progression of systemic lupus and eventual kidney damage in susceptible animals.

Transient pDC depletion has an immediate inhibitory effect on the activation and expansion of both innate and adaptive immune cells during the onset of lupus

To assess the immediate effects of pDC ablation we analyzed 11–wk-old mice at the conclusion of DT treatments (Fig. 7 A). We observed that beneficial effects of pDC ablation were apparent at this early time point. In 11–wk-old lupus-prone mice, we found a significant reduction in the organ weight and cellularity in the absence of pDCs (Fig. 7 B). As seen at later stages of disease, the reduced cellularity was primarily due to diminished CD4+ T cell and CD19+ B cell populations (Fig. 7 C). As seen in 19-wk-old animals, we observed an increased frequency of CD8+ T cells in pDC-depleted mice relative to pDC-sufficient BXSB.DTR male littermate mice, which rescued the population and resulted in equivalent overall numbers of these cells among the mice (unpublished
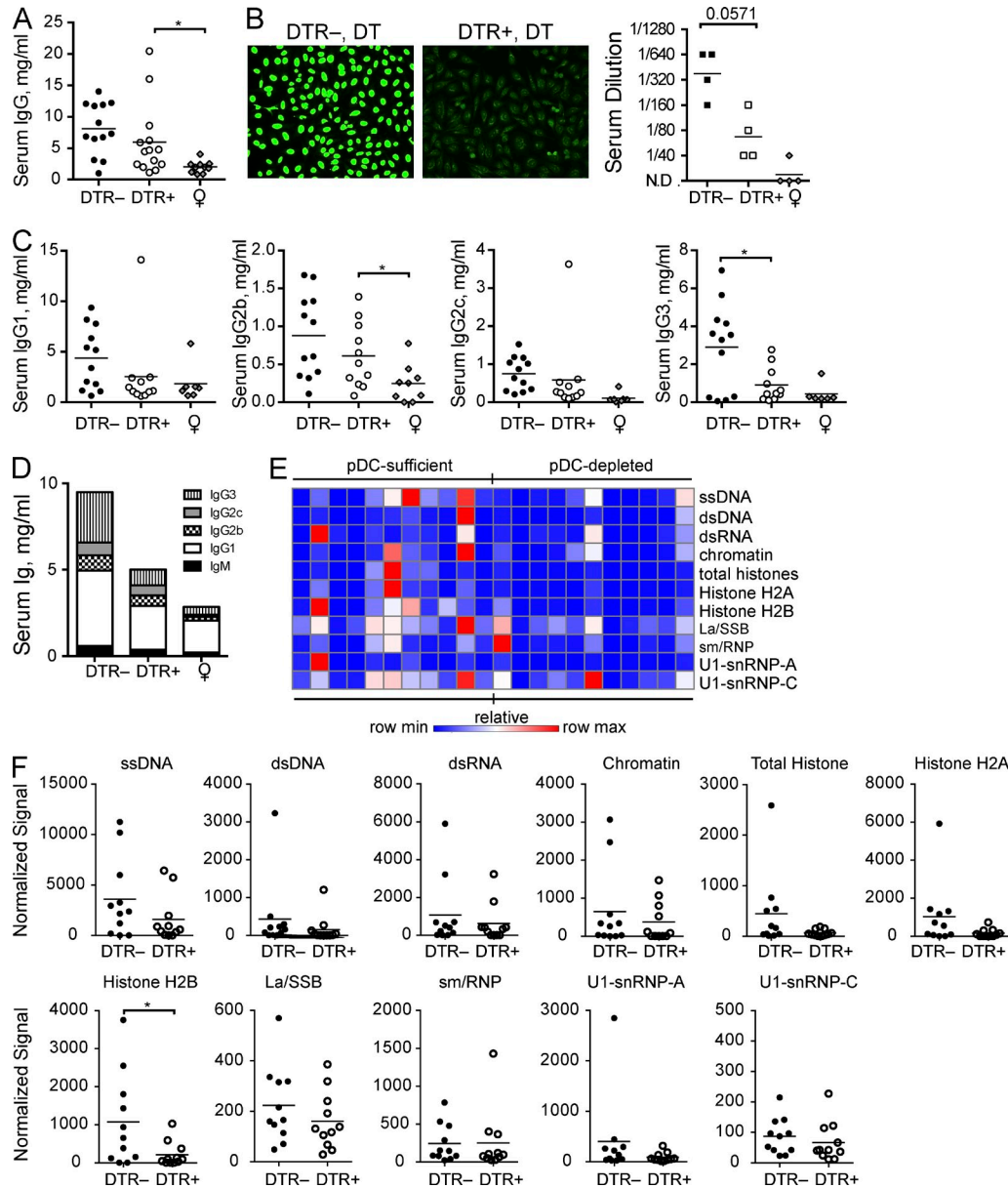
Figure 4. Antinuclear antibodies are reduced in BXSB.DTR mice after transient pDC depletion. Male DTR+ and DTR− mice were treated with DT and analyzed at 19 wk of age. Untreated, healthy female littermates are shown. (A) Total IgG concentration in serum of indicated mice. (B) Antinuclear antibodies in sera were analyzed by HEp-2 assay. (left) Representative images are shown; (right) serum ANAs were titered to endpoint and Mann-Whitney test was applied. N.D. indicates signal was not detected at 1:40 dilution. (C) Concentration of IgG isotypes in serum of indicated mice was determined by ELISA. (D) Mean total serum immunoglobulin concentrations in indicated mice. (E) Sera from 19-wk-old male mice were subjected to an autoantigen microarray. Heat map of IgG antibody reactivity to indicated autoantigens in pDC-sufficient (BXSB.DTR−, DT) and pDC-depleted (BXSB.DTR+, DT) mice is shown. Each column represents an individual mouse; each row indicates a single antigen. Relative maximum row signals are shown in red; relative minimum row signals are shown in blue. (F) Normalized signal of serum IgG reactivity for indicated antigens, as analyzed by autoantigen microarray described in (E). Data points indicate individual mice grouped from 10 experiments. Bar indicates arithmetic mean. *, P < 0.5; **, P < 0.01; ***, P < 0.001. Absence of * indicates nonsignificant differences.

data). We also observed reduced activation of CD4+ and CD8+ T cells, as measured by CD44, CD62L, and CD69 expression (Fig. 7, D–F). In addition, we found that the population of B cells expressing the activation marker CD86 was reduced in the spleens of 11-wk-old pDC-depleted animals (Fig. 7 G). In 11-wk-old mice, there was also a significant reduction in the DC compartment; both CD11b$^{low/-}$CD11c^{high} and CD11b$^+$CD11c^{high} DC subset numbers were decreased after early ablation of pDCs (Fig. 7 H). Thus, the major hallmarks of immune activation were less evident in mice immediately after pDC depletion, which correlated with less severe end-point pathology in these animals.
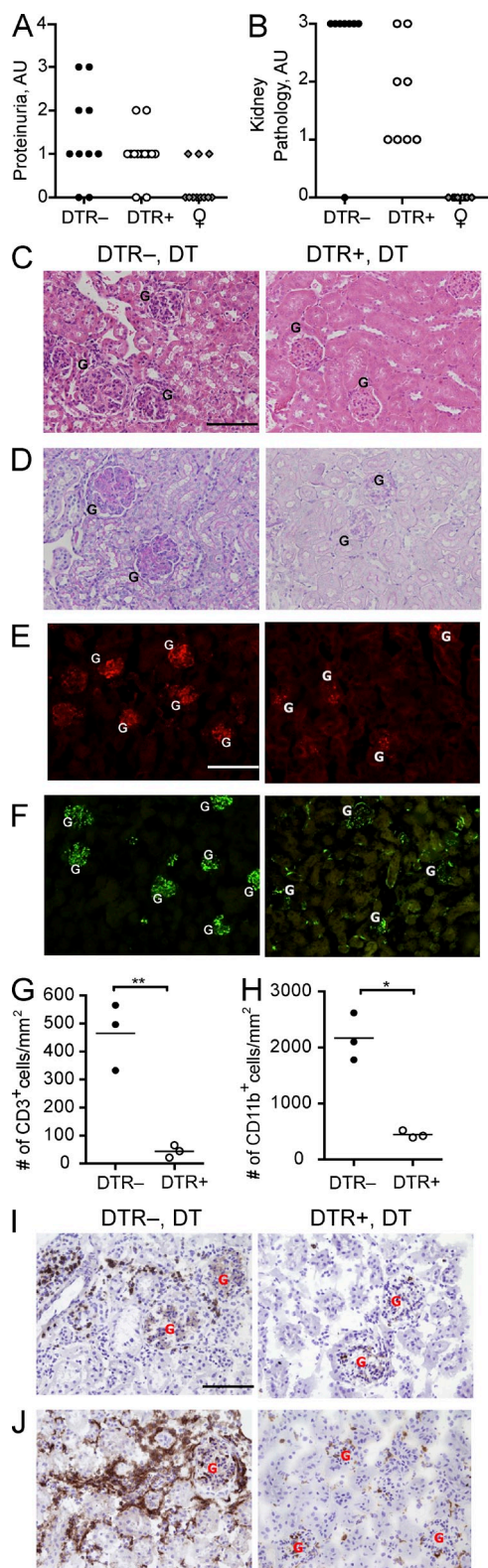
Analysis of IFN-α/β–stimulated genes in 11-wk-old mice indicated that the lupus-associated IFN-α/β gene signature was markedly attenuated after early pDC depletion. Expression of IFN-α/β gene targets was reduced in the peripheral blood of 11-wk-old pDC-depleted mice (Fig. 7 I). Together, these findings indicate an early role for IFN-α/β in the initial expansion and activation of both innate and adaptive immune cells during the onset of lupus, which is likely mediated by the activity of pDCs.

Early, transient pDC depletion has an immediate inhibitory effect on autoantibody production

We analyzed the effect of early pDC ablation on the serum antibody profiles in 11-wk-old BXSB.DTR littermates at the conclusion of DT treatments. Similar to 19-wk-old animals, we observed a significant reduction in the abundance of circulating IgG and IgM in the serum of pDC-depleted mice (Fig. 8, A and C). Again, serum immunoglobulins were reduced across all IgG subclasses (Fig. 8, B and C). As before, we performed a qualitative analysis to screen the specificities of serum antibodies by autoantigen array. We found a striking difference in the autoantibody repertoires of DT-treated BXSB.DTR[-] and BXSB.DTR[+] animals analyzed at 11 wk of age. We observed reduced autoantibody reactivity to a wide variety of autoantigens, including many that are commonly associated with human lupus. Indeed, we found that antibody recognition of the lupus-associated antigens dsDNA, ssDNA, dsRNA, U1-snRNPs, La/SSB, chromatin, and histones were significantly reduced in the serum of mice that were previously depleted of pDCs (Fig. 8, D and E). Overall, these data indicate that transient pDC depletion limits, or delays, the early production of autoantibodies in lupus-prone mice.

Transient pDC depletion leads to reduced expression of lupus–associated soluble factors and inflammatory chemokines

We performed protein arrays to assess any changes in the expression of soluble factors that may mediate protection against the progression of lupus or indicate potential new biomarkers for disease. We screened sera samples from pDC-sufficient or pDC-depleted 11- and 19-wk-old BXSB.DTR mice using a multianalyte platform. Interestingly, we found less soluble VCAM-1 in pDC-deficient animals at both 11 and 19 wk of

PAS (D). Images are representative of four to eight animals per group. Frozen kidney sections were stained for IgG (E, red) and C3 (F, green) to identify immune complexes. Relative abundance of infiltrating CD3^{+} (G) and CD11b^{+} (H) cells in kidney of indicated mice were calculated. Images are representative of three animals per group. Frozen kidney sections were stained for (I) CD3 and (J) CD11b expression. Images are representative of three animals per group. Individual glomeruli are marked in histology panels with the letter G. The magnification in C–F and I–J is 200×. Bars: (C, E, and I) 100 µm. Data points indicate individual mice from three experiments. *, P < 0.5; **, P < 0.01; ***, P < 0.001. Absence of * indicates nonsignificant differences.

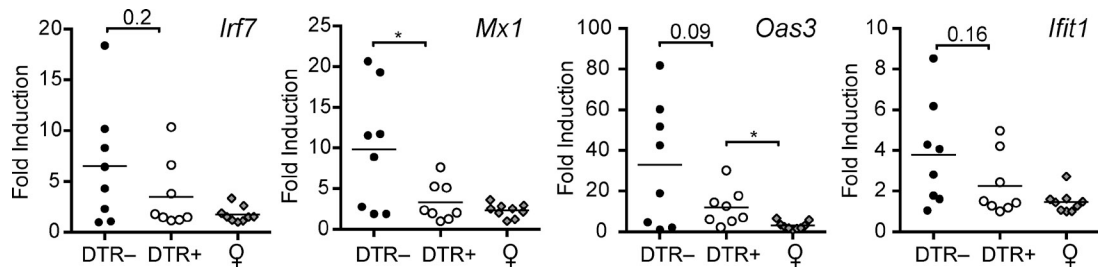**Figure 5.   Early pDC depletion reduces severity of kidney pathology in BXSB.DTR mice.** Male DTR[+] and DTR[-] mice were treated with DT and analyzed at 19 wk of age. Untreated, healthy female littermates are shown. Proteinuria (A) and glomerulonephritis (B) were assessed in indicated mice. Formalin-fixed kidney sections were stained with H&E (C) or

Figure 6.   Local expression of IFN-α/β–stimulated genes in kidney tissues is reduced after pDC depletion. Male DTR[+] and DTR[−] mice were treated with DT and analyzed at 19 wk of age. Untreated, healthy female littermates are shown. Relative expression of indicated genes in kidney tissue was analyzed by RT-PCR. Data points indicate individual mice grouped from eight experiments. Bar indicates mean relative expression of indicated genes. *, P < 0.5; **, P < 0.01; ***, P < 0.001. Absence of * indicates nonsignificant differences.

age (Fig. 9 A). Soluble VCAM-1 is increased in human SLE patients relative to healthy controls and has been correlated with disease severity (Spronk et al., 1994; Ikeda et al., 1998; Howe et al., 2012). We also detected reduced soluble CD40L in the serum of pDC-depleted BXSB.DTR mice relative to pDC-sufficient littermates (Fig. 9 B). Higher levels of soluble CD40L have also been reported in serum of SLE patients (Kato et al., 1999; Vakkalanka et al., 1999; Goules et al., 2006), and may contribute to the activation of autoreactive B cells in lupus.

Although we saw no difference in the population of neutrophils in pDC-depleted BXSB.DTR mice relative to lupus-controls (unpublished data), we found increased levels of circulating myeloperoxidase (MPO) in the serum of pDC-sufficient lupus control animals (Fig. 9 C). Human lupus patients reportedly have higher levels of MPO in plasma compared with healthy controls (Telles et al., 2010). Thus, although neutrophil populations were similar between the groups, enhanced MPO production in pDC-sufficient BXSB.DTR[−] may indicate a difference in the activation status or function of these cells relative to pDC-depleted animals.

Additionally, we observed increased concentrations of the inflammatory chemokines MIP-1β/CCL4, MIP-1γ/CCL9, and MCP-3/CCL7 in the serum of male pDC-sufficient BXSB.DTR mice relative to pDC-depleted littermates and healthy female controls (Fig. 9 D). Prior studies have noted that these proteins are expressed in human lupus patients and correlate with disease severity (Vilá et al., 2007; Bethunaickan et al., 2012; Santer et al., 2012). Thus, considered in the context of previous studies, our findings support a role for pDCs in the induction of inflammatory chemokines during lupus.

DISCUSSION
Although pDCs were implicated in the pathogenesis of SLE some time ago, data supporting this conclusion are primarily correlative; the direct effects of pDCs on lupus have not been thoroughly investigated in vivo. In this study, we generated a novel mouse strain, BXSB.DTR, to selectively evaluate the contribution of pDCs to the progression of lupus in vivo. We find that the early, transient elimination of pDCs is sufficient to improve many of the clinical symptoms of lupus in the BXSB.DTR strain, including reduced expansion and activation

of innate and adaptive immune cells, as well as diminished end-point renal pathology and autoantibody production. Our data indicate an important role for pDCs during the onset of lupus, as early pDC depletion curbed activation of the host immune response in lupus-prone mice as young as 11 wk of age. Importantly, the effects of transient, early pDC ablation were sustained and pathology was minimal at 19 wk of age, at which time the mice normally develop overt disease. Even though the population of pDCs returns to normal once treatment with DT is discontinued, the recovered pDCs appear to have minimal contributions to disease pathogenesis at later stages of disease, again illustrating an important role for pDCs in the early activation of other immune cells.

The early contribution of pDCs to lupus pathogenesis is likely mediated, at least in part, by the production of IFN-α/β. We found a much less marked IFN-α/β–induced gene signature in the blood of young pDC-depleted mice, which correlated with reduced local gene expression in the tissues of older pDC-depleted mice. It was recently reported that chronic treatment of BXSB mice with an anti-IFNAR–blocking antibody improved clinical signs of lupus (Baccala et al., 2012), indicating an important role for IFN-α/β in the pathogenesis of lupus. In this study, lupus symptoms were more effectively ameliorated when treatment with anti-IFNAR antibodies was initiated in younger BXSB mice rather than in older mice, after the onset of disease. The reduced efficacy of IFNAR blockade after disease onset, when activation of the adaptive immune response has already occurred, bolsters our view that pDCs and IFN-α/β may play a less significant role in sustaining pathogenesis at later stages of disease. However, our results do not exclude the potential effects of other inflammatory mediators produced by pDCs, such as IL-6, which was previously reported to facilitate plasma cell differentiation by acting in combination with IFN-α/β (Jego et al., 2003).

Our data suggest that pDCs control the early threshold activation of adaptive immune cells and accelerate the progression of lupus. CD4^{+} T cells are reportedly involved in the pathogenesis of lupus, potentially by providing signals for B cell activation. Indeed, an increased frequency of activated antigen experienced CD44^{high} CD4^{+} T cells has been reported in BXSB mice (Chu et al, 1994). We found fewer activated T cells
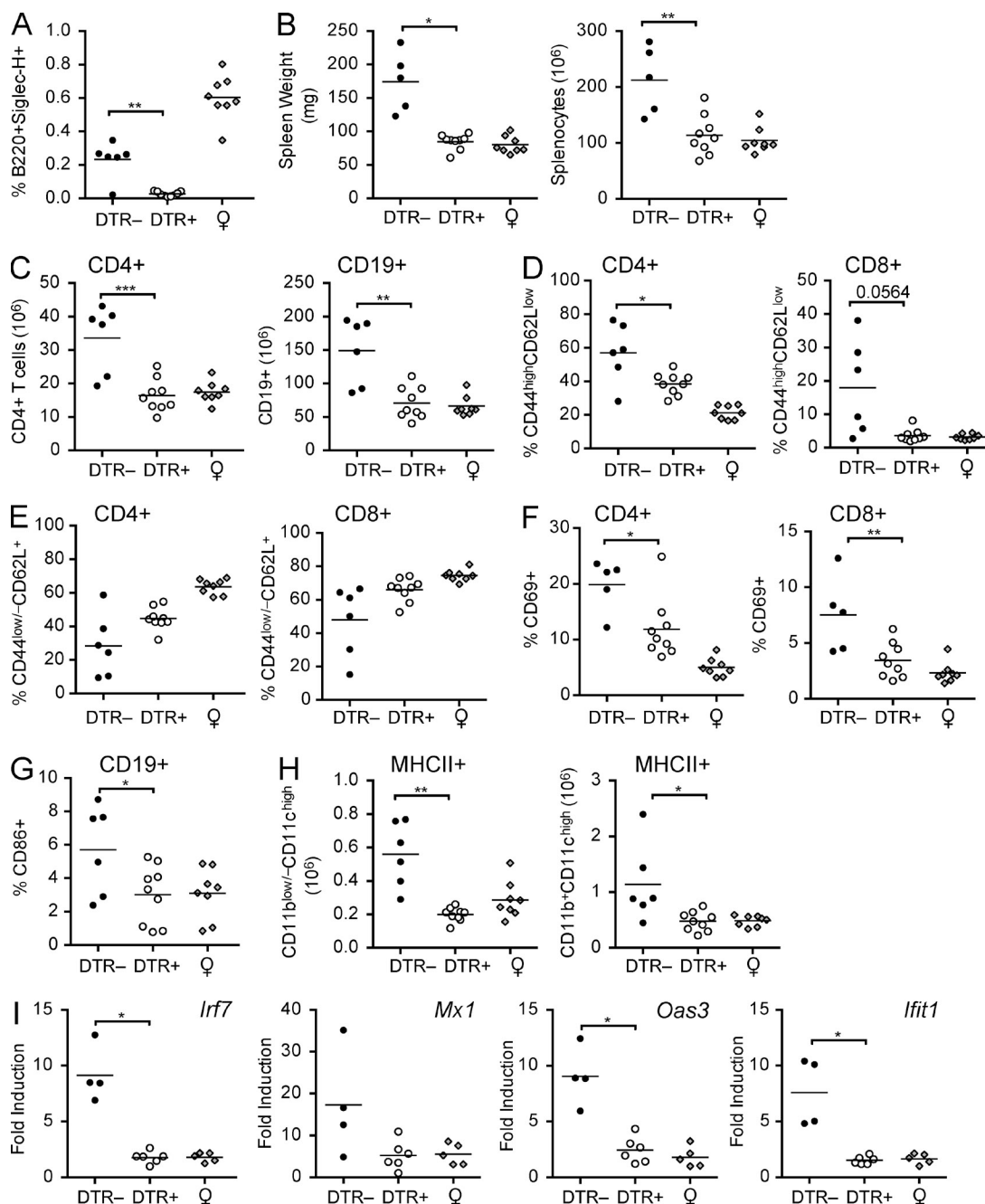
Figure 7. Transient pDC depletion has an immediate effect on the activation and expansion of innate and adaptive immune cells. Male mice were treated with DT and analyzed at 11 wk of age. Untreated, healthy female littermates are shown. (A) Frequencies of B220+SiglecH+ pDCs 24 h after last DT treatment were determined by flow cytometry. (B) Spleen weight and absolute cell number were calculated in indicated mice. (C) Number of CD4+ and CD19+ splenocytes. Frequencies of CD44highCD62Llow (D), CD44low/-CD62L+ (E), and CD69+ CD4+ and CD69+CD8+ (F) T cells in spleen of indicated mice. (G) Frequencies of CD86+CD19+ splenocytes. (H) Number of CD11blow/-CD11chigh and CD11b+CD11chigh MHCII+ DCs in spleen of indicated mice. (I) Relative expression of indicated IFN-α/β–induced genes in peripheral blood was analyzed by RT-PCR. Data points indicate individual mice. Bar indicates arithmetic mean. *, P < 0.5; **, P < 0.01; ***, P < 0.001. Absence of * indicates nonsignificant differences.

expressing CD44 and CD69 in the spleens of BXSB mice that were subjected to early pDC depletion. We also noticed pDC-depleted mice had a remarkable reduction of kidney infiltrating CD3+ T cells, which reportedly promote nephritis in lupus-prone MRL/lpr mice (Okamoto et al., 2012). This

further suggests that early activity of pDCs in BXSB mice promotes aberrant T cell activation and T cell trafficking to the kidneys. The study by Baccala et al. (2012) also reported a reduced frequency of CD4+ and CD8+ T cells expressing CD69 in BXSB mice undergoing chronic treatment with a
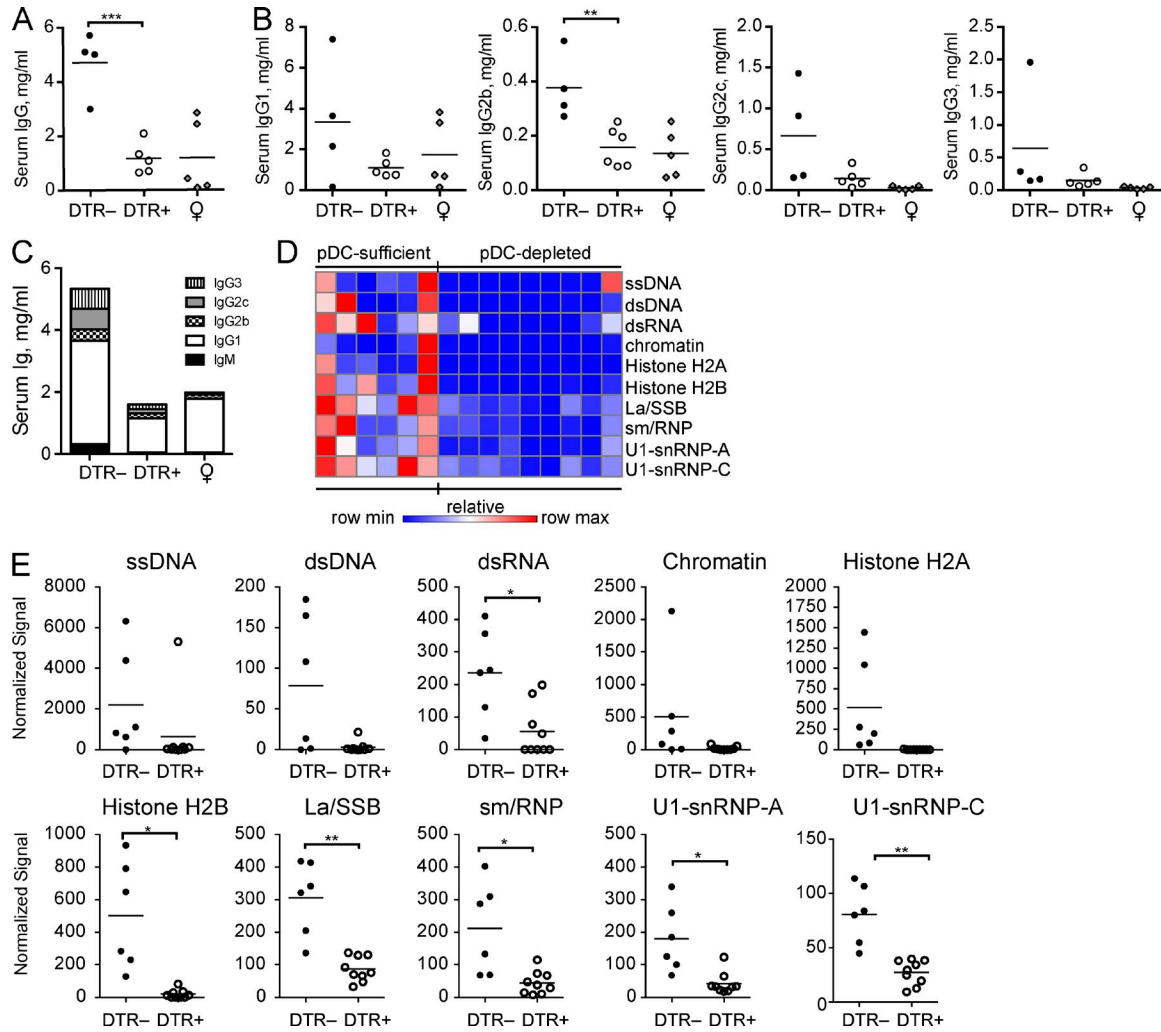
Figure 8. Transient pDC depletion has an immediate effect on the presence of circulating autoantibodies. Male DTR[+] and DTR[−] mice were treated with DT and analyzed at 11 wk of age. Untreated, healthy female littermates are shown. (A–C) Total IgG concentration in serum (A), individual IgG isotypes (B), and mean total serum IgG concentration (C) was determined by ELISA in the indicated mice. (D) Sera from 11-wk-old male mice were subjected to an autoantigen microarray. Heat map of IgG antibody reactivity to indicated autoantigens in pDC-sufficient (BXSB.DTR−, DT) and pDC-depleted (BXSB.DTR+, DT) mice. Each column represents an individual mouse; each row indicates a single antigen. Relative maximum row signals are shown in red; relative minimum row signals are shown in blue. (E) Normalized signal of serum IgG reactivity for indicated antigens, as analyzed by autoantigen microarray described in (D). Serum autoantibodies (IgG) were analyzed by autoantigen microarray as in (D) and normalized signals for the indicated antigens are shown. Data points represent individual mice. Bar indicates arithmetic mean. *, P < 0.5; **, P < 0.01; ***, P < 0.001. Absence of * indicates nonsignificant differences.

blocking antibody against IFNAR. Furthermore, we observed soluble CD40L in serum of 19-wk-old pDC-sufficient BXSB mice, which provides additional evidence of prior T cell activation. Soluble CD40L detected in sera of human SLE patients correlated with disease severity and may contribute to B cell activation (Kato et al., 1999; Vakkalanka et al., 1999; Goules et al., 2006). Together, these data suggest that T cell activation in the BXSB model is downstream of pDC–IFN-α/β axis. We have not determined whether the effects of pDCs on T cell responses are mediated directly by production of cytokines by pDCs or indirectly, perhaps by activation of intermediate cells such as conventional DCs (cDCs) or B cells. We found differences in cDC populations immediately after pDC depletion, which suggests that these cells may participate

in downstream adaptive immune system responses. For the MRL.Fas[lpr] model of lupus, it has been reported that cDCs are important for the expansion and differentiation of T cells, however not for their initial activation (Teichmann et al., 2010). Thus, we cannot dismiss that a direct effect of pDCs on T cells, or on other antigen-presenting cells, such as B cells, are important for the initial activation of T cells.

Several results indicate that pDCs may also have a crucial role in promoting abnormal B cell responses in lupus. We find that early pDC depletion results in the reappearance of MZ B cells, which are absent from BXSB mice with active signs of lupus (Amano et al., 2003). MZ B cells are thought of as innatelike B cells that function in the nonspecific, but rapid, defense against blood borne pathogens by secreting
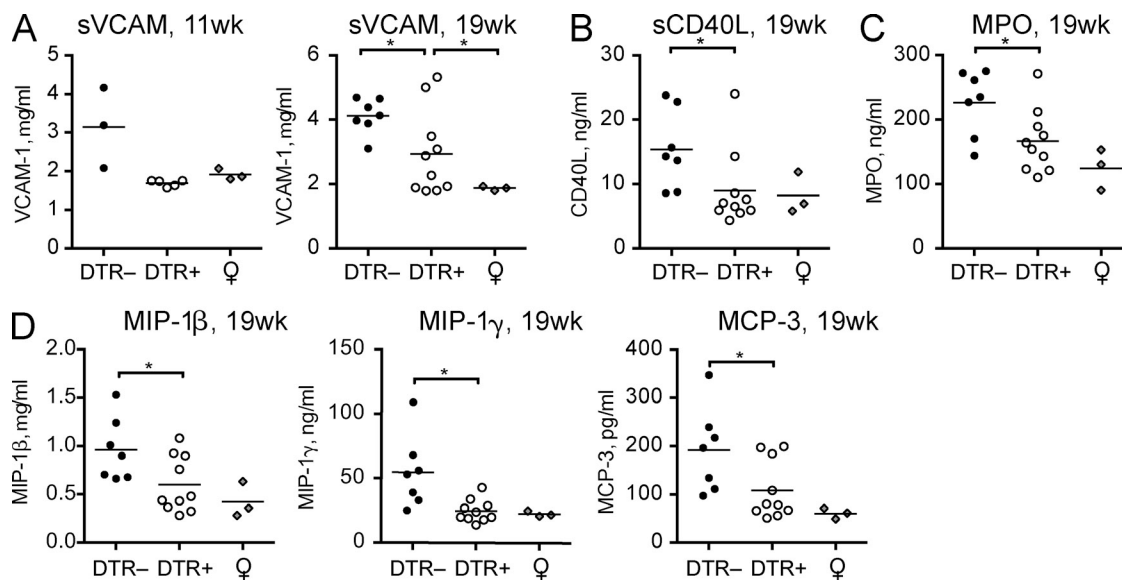
Figure 9. Reduced lupus–associated soluble factors and inflammatory chemokines in sera after early pDC depletion. Male DTR[+] and DTR[−] mice were treated with DT and analyzed at 11 or 19 wk of age, as marked. Age-matched, untreated, healthy female littermates are included. Concentration of soluble (A) VCAM-1, (B) CD40L, (C) MPO, and (D) select chemokines in sera of indicated mice were determined by serum protein array. Data points indicate samples from individual mice analyzed by MyriadRBM rodent MAPv3.0 array. *, $P < 0.5$; **, $P < 0.01$; ***, $P < 0.001$. Absence of * indicates nonsignificant differences.

antibodies with broad reactivity (Cerutti et al., 2013). Although the disappearance of MZ B cell compartment in BXSB mice is incompletely understood, it may indicate the differentiation of MZ B cells into autoantibody-secreting plasma cells. We also find that transient, early depletion of pDCs limited the development of ABCs, an unusual population of B cells that were shown to accumulate with age in normal mice and were also found in young autoimmune prone animals as well as in patients with systemic autoimmunity (Hao et al., 2011; Rubtsov et al., 2011). The accumulation of these cells is dependent on TLR7 signaling (Hao et al., 2011; Rubtsov et al., 2011). In addition, the ABC population is diminished after blockade of the IFNAR (Baccala et al., 2012). These data suggest that the activity of pDCs early during the onset of autoimmunity promotes the dysregulated development of B cells into ABCs and this is likely due, at least in part, to the action of IFN-α/β on B cells.

We did not detect any differences in the population of plasma cells in BXSB.DTR mice, regardless of early pDC depletion. Although there was no change in the CD138^{+} plasma cells, we did observe a reduction in total serum immunoglobulin titers and autoantibodies after pDC depletion. Serum immunoglobulins were reduced across all IgG isotypes. BXSB.DTR mice that were depleted of pDCs had reduced autoantibodies against nuclear antigens. Thus, it is possible that although the frequency of plasma cells is unchanged, there is a shift in the repertoire of antibodies that are produced in mice depleted of pDCs. It may be that the early production of IFN-α/β by pDCs skews the B cell population toward having a more autoreactive BCR repertoire or affects the antibody production by these cells. Indeed, we found decreased overall titers of antinuclear autoantibodies (ANAs) in

serum of pDC-depleted mice, as quantified by HEp-2 assay. In complementary, qualitative array assays we found reduced antibody reactivity against several lupus–associated autoantigens, primarily in 11-wk-old BXSB.DTR mice immediately after pDC depletion. These data suggest an immediate effect of pDC depletion on inhibiting, or delaying, the production of autoantibodies. By qualitative array assay, the differences in self-antigen recognition were less dramatic in 19-wk-old animals, with only reactivity to Histone H2B showing a significant difference. The observation that this effect waned over time may indicate that pDCs are important for induction of disease, and in their absence the progression of lupus is delayed, but not completely abolished. However, it is important to note that the autoantigen arrays were performed using a single, standard serum dilution, which may not be optimal for all the samples given the differences in total serum Ig concentrations between pDC-sufficient and pDC-depleted animals. For this reason, it is possible that differences in antigen binding may be underestimated in the 19-wk-old animals, when overall serum Ig concentrations are higher relative to that seen in younger mice. Based on the serum concentrations and ANA titers, we conclude that transient pDC-depletion limits the production of autoantibodies in lupus-prone mice.

Additionally, we found evidence that pDC depletion reduced the expression of several soluble proteins that may be relevant to the progression of lupus. We observed lower levels of soluble VCAM-1 (sVCAM-1) in BXSB.DTR mice that were previously depleted of pDCs. sVCAM-1 is found at higher levels in the serum and urine of human SLE patients relative to healthy controls and correlates with disease severity, including autoantibody production and incidence of lupus nephritis (Spronk et al., 1994; Ikeda et al., 1998; Howe et al.,

2012). Increased sVCAM-1 may indicate prior activation of endothelial cells, perhaps as a result of immune complex deposition and complement activation, which could facilitate the migration of inflammatory cells into tissues.

We also observed that mice previously depleted of pDCs had reduced expression of the inflammatory chemokines MIP-1β, MIP-1γ, and MCP-3. Interestingly, human lupus patients are reported to have higher serum concentrations of MIP-1β than healthy individuals, which correlate with tissue damage in SLE (Vilá et al., 2007). MIP-1γ is found only in rodents (human orthologue MIP-1δ/CCL15), but lower levels of MIP-1γ were found to correlate with less severe lupus nephritis in a murine model (Bethunaickan et al., 2012). Maximal induction of MCP-3 in response to immune complexes from lupus serum was reported to be dependent on pDCs (Santer et al., 2012), a finding supported by the reduced expression of MCP-3 we noted after pDC depletion.

The role of pDCs in lupus in vivo has been indirectly studied using IRF8-deficient mice. It was concluded that pDCs are critical for the pathogenesis of lupus based on the limited production of autoantibodies against nuclear antigens (Baccala et al., 2013). In the same study, the phenotype of IRF8-deficient mice was similar to that of Slc15a4-deficient mice, which harbor pDCs that have impaired production of IFN-α/β and inflammatory cytokines (Blasius et al., 2010). Although our data are in strong agreement that pDCs are important in lupus, our system represents an improved model for studying pDCs in vivo, as IRF8-deficient mice also have defects in CD8α+ cDCs and IL-12 (Aliberti et al., 2003), whereas Slc15a4 is also expressed in B cells and therefore Slc15a4-deficient mice may have B cell intrinsic defects. As such, the nonspecific deletion of additional cell types may result in a more dramatic phenotype. Thus, although our data are in agreement with some published studies, our model provides a more specific and physiologically relevant evaluation of the impact of pDCs in systemic autoimmunity.

In conclusion, we have identified pDCs to be a critical cell type responsible for the pathogenesis of lupus. We demonstrate that the early activity of this cell type contributes to induce full disease symptoms via the activation of T cells, B cells, and cDCs. Our observation that the frequency of pDCs returns to normal in BXSB.DTR+ mice after DT treatment is stopped, yet protection from disease is sustained, implies that the pathogenic activity of pDCs is principally important during a limited window early in disease progression, at which time they are able to initiate the activation of other immune cell types. We cannot entirely dismiss a contribution of pDCs at later stages of disease; however, it is most likely that pDCs are less important once a threshold level of cell activation has been achieved, as we see a significant delay in the progression of lupus after a limited period of pDC ablation. Our work suggests that transient short-term depletion of pDCs may represent an attractive therapeutic approach for the early treatment of lupus by inhibiting the activation of autoreactive T and B cells while leaving the antiviral responses and IFN-α/β pathway intact in all other cell types.

MATERIALS AND METHODS

Mice and treatments. BXSB/MpJ mice were obtained from The Jackson Laboratory. C57BL/6-Tg(CLEC4C-HBEGF)956Cln Tg mice (BDCA2-DTR Tg mice) have been described (Swiecki et al., 2010). BXSBxBDCA2-DTR mice were generated by breeding male BXSB/MpJ to female BDCA2-DTR mice, selecting for BXSB susceptibility loci on Chromosome 1 during the initial backcrosses (Haywood et al., 2006). To distinguish them from the parental BxSB/MpJ strain, all mice from the line generated by backcrossing the BDCA2-DTR transgene to BXSB/MpJ will be referred to as BXSB.DTR mice (Tg+ BXSB.DTR+ and Tg− BXSB.DTR− mice will only be distinguished when necessary). Female BXSB.DTR+ mice were bred to male BXSB/MpJ mice for all subsequent backcrosses, producing DT-responsive BXSB.DTR+ and DT-nonresponsive BXSB.DTR− littermate mice for all experiments. Experimental mice were used at backcross generation N11-N14. Plasmacytoid DCs were depleted in BXSB.DTR+ mice by i.p. administration of 100 ng DT (Sigma-Aldrich) every 3–4 d for 3 wk beginning when mice were 8 wk of age. PDC-sufficient control BXSB.DTR− littermates were injected with DT, and both BXSB.DTR+ and BXSB.DTR− mice were treated with PBS in parallel experiments (SLE controls). Mice were housed under specific pathogen-free conditions and animal protocols were approved by the Animal Studies Committee at Washington University in Saint Louis.

Isolation of leukocytes. Whole blood was collected via cardiac puncture at time of sacrifice. Bone marrow cells were flushed with RPMI 1640 containing 10% bovine calf serum (RPMI-10%). Spleens and lymph nodes were minced and digested with Collagenase D (Roche) for 45 min at 37°C in RPMI-10%. Spleen and lymph node tissues were pressed through nylon mesh strainers (BD) to yield single-cell suspensions. Red blood cells were removed from spleen and bone marrow with RBC lysis buffer (Sigma-Aldrich). Cells were counted by hemacytometer using Trypan Blue to exclude dead cells.

Flow cytometric analysis. Single-cell suspensions were stained with fluorescent monoclonal antibodies against B220 (RA3-6B2), CD3 (145.2c11), CD4 (GK1.5 or RM4-5), CD8a (53–6.7), CD11b (M1/70), CD11c (N418), CD19 (1D3), CD23 (B3B4), CD21/35 (7G6), CD93 (AA4.1), CD44 (IM7), CD62L (Mel14), CD86 (GL1), CD138 (281–2), FoxP3 (FJK-16a), Ki-67 (B56), SiglecH (551), CD69 (H1.2F3), IA/IE (2G9 or M5/114.14.2), purchased from BD, eBioscience, or BioLegend. Biotinylated antibodies were revealed with fluorochrome conjugated streptavidin (Invitrogen). Before staining, cells were treated for 10–15 min at room temperature with monoclonal antibody 197 (anti-mFcγRI) to block Fc receptors, and dead cells were excluded during FACS analysis with addition of propidium iodide or 7AAD. Intracellular FoxP3 expression was analyzed according to manufacturer's instructions (eBioscience) after surface marker staining. Staining for Ki67 expression was sometimes included with FoxP3 analysis. Data were acquired on a FACS-Canto II (BD) and analyzed using FlowJo software (Tree Star, Inc.).

ELISAs. Sera were isolated from whole blood using serum collection tubes (BD) and stored at −20°C until use. Microtiter plates were coated overnight with 2 µg/ml goat anti–mouse IgG (Southern Biotech) diluted in PBS at 4°C. Plates were washed once (PBS, 0.1% Tween-20), blocked 2 h at 37°C or 4°C overnight (PBS, 1% BSA), and again washed once. Sera were initially diluted 1:1,000 (IgG and IgM) or 1:500 (IgG isotypes), serially diluted threefold in blocking buffer, and incubated overnight at 4°C. Standard curves were generated using known concentrations of purified antibodies. Plates were washed three times and bound antibodies were detected with horseradish peroxidase (HRP)-conjugated goat anti–mouse IgM, IgG, IgG2b, and IgG2c isotype-specific antibodies (1:500; Southern Biotech), HRP-goat anti–mouse IgG1 (1:1,000; Invitrogen) or HRP-rabbit anti–mouse IgG3 (1:1,000; Rockland) for 1 h at 37°C. Plates were washed three times, and developed by adding peroxidase substrate buffer comprised of 1 mg/ml o-phenylenediamine dihydrochloride (Sigma-Aldrich) diluted in 0.05 M phosphate citrate buffer, pH 5.0. Absorbance values were read at 490 nm.

Antinuclear antibody assays. Serum samples were prepared by diluting in PBS. Diluted samples were applied to HEp-2 cell–coated slides (MBL Bion) and incubated 1 h at room temperature in a humidified chamber. Slides were washed 3 times in PBS. Bound antibodies were detected after incubation with Alexa Fluor 488-conjugated F(ab′) goat anti–mouse IgG (Invitrogen) diluted 1:200 in PBS for 1 h at room temperature in a humidified chamber. Slides were washed 3 times (5 min each) in PBS and images were visualized on a Nikon Eclipse E800 microscope equipped with a 60×/1.4 numerical aperture oil objective. Images were captured using a Magnafire camera (Optronics) and processed using Nikon Elements and ImageJ (National Institutes of Health) software. ANA titers are represented as highest dilution of serum that contained detectable autoantibodies. Additionally, serum autoantibodies were evaluated using the Autoantigen Microarray Panel I at the Genomics and Microarray Core Facility (University of Texas Southwestern, Dallas, TX). Subsequent analyses of normalized signals were completed using GraphPad prism 6.0. Fluorescence intensities in heat maps that were higher than the row mean were shown in red; those below than the row mean were shown in blue; those near the mean were shown in white.

Serum protein arrays. Murine serum samples were evaluated and quantified using the RodentMAP v.3.0 multi-analyte platform (Myriad RBM). Samples with undetectable protein were assigned values equivalent to the individual assay LLOQ. Heat maps were generated using GENE-E online software (http://www.broadinstitute.org/cancer/software/GENE-E/).

Tissue pathology and histological analysis. Kidneys were either fixed in 10% neutral buffered formalin and sections were stained for hematoxylin and eosin (H&E) and Periodic acid-Schiff (PAS) by the Anatomical and Molecular Pathology Laboratory at Washington University (St. Louis). Fixed sections were blindly scored on a scale of 0–3 for increasing severity of glomerulonephritis (GN) per the following scale: (1) minimal damage to glomerular basement membranes (GBM) and little to no cellular infiltrates; (2) intermediate degree of cellular infiltration with moderate damage to GBM; (3) extensive cellular infiltration and severe destruction of GBM, which may include presence of casts indicating proteinuria. For immunohistochemistry, kidneys were frozen in OCT compound and cryostat sections (5 µm in thickness) were stained with CD3 (rabbit monoclonal, clone SP7, dilution 1:100; Thermo Fisher Scientific), CD11b (rat IgG2b, clone M1/70, dilution 1:100; BD), Gr-1 (rat IgG2b, clone RB6-8C5, dilution 1:100), and 440c (rat IgG2b, dilution 1:50). Reactivity was detected using EnVision Rabbit (Dako) or Rat-on-Mouse HRP-Polymer kit (Biocare Medical), followed by diaminobenzidine as chromogen and hematoxylin as counterstaining. For immunofluorescence, sections were stained with fluorescein–conjugated goat F(Ab')₂ Fragment to Mouse Complement C3 (dilution 1:800; MP Biomedical) and with a Cy™3-conjugated AffiniPure F(Ab')₂ Fragment Donkey Anti–Mouse IgG (H+L) (dilution 1:800; Jackson ImmunoResearch Laboratories) and counterstained with DAPI. The density of T cells and myeloid cells infiltrating the kidney tissue was defined by automatic cell counting on digitalized slides (Aperio Scanscope, Nuclear algorithm) obtained from sections immunostained with CD3 and CD11b.

Measurement of Proteinuria. Urine was collected 1–2 d before sacrifice and proteinuria quantified using Albustix strips (Bayer) and semiquantitative scores were assigned based on colorimetric scale. (0, negative to trace; 1, 30 mg/ml; 2, 100 mg/ml; 3, 300 mg/ml; 4, ≥2,000 mg/ml).

RT-PCR. Spleen and kidney samples were flash frozen in liquid nitrogen and stored at −80°C. Whole blood was obtained by cardiac puncture and immediately transferred to RNeasy Protect Animal Blood tubes (QIAGEN). After 2 h at RT, blood was stored at −80°C. According to the manufacturer's recommendation, RNA was extracted from blood using the RNeasy Animal Blood Protect kit (QIAGEN), whereas RNA was extracted from spleen and kidneys using the RNeasy Fibrous Tissue Mini kit (QIAGEN). cDNA was amplified using random primers and SuperScript III (Life Technologies). TaqMan analyses were completed on a 7900HT Fast Real-time PCR System (Applied Biosystems) using TaqMan Fast Advanced Master Mix (Life Technologies) and the following gene expression assays (Life Technologies): IFI44 (Mm00505670_m1), MX1 (Mm00487796_m1), OAS3 (Mm00460944_m1), IRF7 (Mm00516793_g1), and 18S endogenous control (Mm03928990_g1). Amplification cycle data were captured and quantified using SDS 2.4 and RQ Manager 1.2.2 (Applied Biosystems), and fold changes were calculated compared with 18S endogenous control. Data were further analyzed using GraphPad Prism 6.

Statistical analysis. Significant differences between any two groups were calculated with Prism software (GraphPad Software, Inc.). Unless noted, statistical significance was assessed using the unpaired two-tailed Student's t test with Welch's correction applied where appropriate. The Mann-Whitney test was applied where indicated. P values <0.05 were considered significant. *, P < 0.05; **, P < 0.01; ***, P < 0.001. Absence of * indicates non-significant differences.

REFERENCES

Aliberti, J., O. Schulz, D.J. Pennington, H. Tsujimura, C. Reis e Sousa, K. Ozato, and A. Sher. 2003. Essential role for ICSBP in the in vivo development of murine CD8alpha + dendritic cells. *Blood.* 101:305–310. http://dx.doi.org/10.1182/blood-2002-04-1088

Amano, H., E. Amano, T. Moll, D. Marinkovic, N. Ibnou-Zekri, E. Martinez-Soría, I. Semac, T. Wirth, L. Nitschke, and S. Izui. 2003. The Yaa mutation promoting murine lupus causes defective development of marginal zone B cells. *J. Immunol.* 170:2293–2301. http://dx.doi.org/10.4049/jimmunol.170.5.2293

Asselin-Paturel, C., A. Boonstra, M. Dalod, I. Durand, N. Yessaad, C. Dezutter-Dambuyant, A. Vicari, A. O'Garra, C. Biron, F. Brière, and G. Trinchieri. 2001. Mouse type I IFN-producing cells are immature APCs with plasmacytoid morphology. *Nat. Immunol.* 2:1144–1150. http://dx.doi.org/10.1038/ni736

Baccala, R., R. Gonzalez-Quintial, R.D. Schreiber, B.R. Lawson, D.H. Kono, and A.N. Theofilopoulos. 2012. Anti-IFN-α/β receptor antibody treatment ameliorates disease in lupus-predisposed mice. *J. Immunol.* 189:5976–5984. http://dx.doi.org/10.4049/jimmunol.1201477

Baccala, R., R. Gonzalez-Quintial, A.L. Blasius, I. Rimann, K. Ozato, D.H. Kono, B. Beutler, and A.N. Theofilopoulos. 2013. Essential requirement for IRF8 and SLC15A4 implicates plasmacytoid dendritic cells in the pathogenesis of lupus. *Proc. Natl. Acad. Sci. USA.* 110:2940–2945. http://dx.doi.org/10.1073/pnas.1222798110

Baechler, E.C., F.M. Batliwalla, G. Karypis, P.M. Gaffney, W.A. Ortmann, K.J. Espe, K.B. Shark, W.J. Grande, K.M. Hughes, V. Kapur, et al. 2003. Interferon-inducible gene expression signature in peripheral blood cells of patients with severe lupus. *Proc. Natl. Acad. Sci. USA.* 100:2610–2615. http://dx.doi.org/10.1073/pnas.0337679100

Banchereau, J., and V. Pascual. 2006. Type I interferon in systemic lupus erythematosus and other autoimmune diseases. *Immunity.* 25:383–392. http://dx.doi.org/10.1016/j.immuni.2006.08.010

Barbalat, R., S.E. Ewald, M.L. Mouchess, and G.M. Barton. 2010. Nucleic Acid Recognition by the Innate Immune System. *Annu. Rev. Immunol.*

Barrat, F.J., T. Meeker, J. Gregorio, J.H. Chan, S. Uematsu, S. Akira, B. Chang, O. Duramad, and R.L. Coffman. 2005. Nucleic acids of mammalian origin can act as endogenous ligands for Toll-like receptors and may promote systemic lupus erythematosus. *J. Exp. Med.* 202:1131–1139. http://dx.doi.org/10.1084/jem.20050914

Båve, U., M. Magnusson, M.L. Eloranta, A. Perers, G.V. Alm, and L. Rönnblom. 2003. Fc gamma RIIa is expressed on natural IFN-alpha-producing cells (plasmacytoid dendritic cells) and is required for the IFN-alpha production induced by apoptotic cells combined with lupus IgG. *J. Immunol.* 171:3296–3302. http://dx.doi.org/10.4049/jimmunol.171.6.3296

Bennett, L., A.K. Palucka, E. Arce, V. Cantrell, J. Borvak, J. Banchereau, and V. Pascual. 2003. Interferon and granulopoiesis signatures in systemic lupus erythematosus blood. *J. Exp. Med.* 197:711–723. http://dx.doi.org/10.1084/jem.20021553

Bethunaickan, R., R. Sahu, Z. Liu, Y.T. Tang, W. Huang, O. Edegbe, H. Tao, M. Ramanujam, M.P. Madaio, and A. Davidson. 2012. Anti-tumor necrosis factor α treatment of interferon-α-induced murine lupus nephritis reduces the renal macrophage response but does not alter glomerular immune complex formation. *Arthritis Rheum.* 64:3399–3408. http://dx.doi.org/10.1002/art.34553

Blasius, A.L., M. Cella, J. Maldonado, T. Takai, and M. Colonna. 2006. Siglec-H is an IPC-specific receptor that modulates type I IFN secretion through DAP12. *Blood.* 107:2474–2476. http://dx.doi.org/10.1182/blood-2005-09-3746

Blasius, A.L., C.N. Arnold, P. Georgel, S. Rutschmann, Y. Xia, P. Lin, C. Ross, X. Li, N.G. Smart, and B. Beutler. 2010. Slc15a4, AP-3, and Hermansky-Pudlak syndrome proteins are required for Toll-like receptor signaling in plasmacytoid dendritic cells. *Proc. Natl. Acad. Sci. USA.* 107:19973–19978. http://dx.doi.org/10.1073/pnas.1014051107

Cerutti, A., M. Cols, and I. Puga. 2013. Marginal zone B cells: virtues of innate-like antibody-producing lymphocytes. *Nat. Rev. Immunol.* 13:118–132.

Chu, E.B., D.N. Ernst, M.V. Hobbs, and W.O. Weigle. 1994. Maturational changes in CD4+ cell subsets and lymphokine production in BXSB mice. *J. Immunol.* 152:4129–4138.

Crow, M.K., K.A. Kirou, and J. Wohlgemuth. 2003. Microarray analysis of interferon-regulated genes in SLE. *Autoimmunity.* 36:481–490. http://dx.doi.org/10.1080/08916930310001625952

Deane, J.A., P. Pisitkun, R.S. Barrett, L. Feigenbaum, T. Town, J.M. Ward, R.A. Flavell, and S. Bolland. 2007. Control of toll-like receptor 7 expression is essential to restrict autoimmunity and dendritic cell proliferation. *Immunity.* 27:801–810. http://dx.doi.org/10.1016/j.immuni.2007.09.009

Dzionek, A., Y. Sohma, J. Nagafune, M. Cella, M. Colonna, F. Facchetti, G. Günther, I. Johnston, A. Lanzavecchia, T. Nagasaka, et al. 2001. BDCA-2, a novel plasmacytoid dendritic cell-specific type II C-type lectin, mediates antigen capture and is a potent inhibitor of interferon α/β induction. *J. Exp. Med.* 194:1823–1834. http://dx.doi.org/10.1084/jem.194.12.1823

Elkon, K.B., and D.M. Santer. 2012. Complement, interferon and lupus. *Curr. Opin. Immunol.* 24:665–670. http://dx.doi.org/10.1016/j.coi.2012.08.004

Fairhurst, A.M., A.E. Wandstrat, and E.K. Wakeland. 2006. Systemic lupus erythematosus: multiple immunological phenotypes in a complex genetic disease. *Adv. Immunol.* 92:1–69. http://dx.doi.org/10.1016/S0065-2776(06)92001-X

Fairhurst, A.M., S.H. Hwang, A. Wang, X.H. Tian, C. Boudreaux, X.J. Zhou, J. Casco, Q.Z. Li, J.E. Connolly, and E.K. Wakeland. 2008. Yaa autoimmune phenotypes are conferred by overexpression of TLR7. *Eur. J. Immunol.* 38:1971–1978. http://dx.doi.org/10.1002/eji.200838138

Farkas, L., K. Beiske, F. Lund-Johansen, P. Brandtzaeg, and F.L. Jahnsen. 2001. Plasmacytoid dendritic cells (natural interferon- alpha/beta-producing cells) accumulate in cutaneous lupus erythematosus lesions. *Am. J. Pathol.* 159:237–243. http://dx.doi.org/10.1016/S0002-9440(10)61689-6

Garcia-Romo, G.S., S. Caielli, B. Vega, J. Connolly, F. Allantaz, Z. Xu, M. Punaro, J. Baisch, C. Guiducci, R.L. Coffman, et al. 2011. Netting neutrophils are major inducers of type I IFN production in pediatric systemic lupus erythematosus. *Sci. Transl. Med.* 3:73ra20. http://dx.doi.org/10.1126/scitranslmed.3001201

Gilliet, M., W. Cao, and Y.J. Liu. 2008. Plasmacytoid dendritic cells: sensing nucleic acids in viral infection and autoimmune diseases. *Nat. Rev. Immunol.* 8:594–606.

Goules, A., A.G. Tzioufas, M.N. Manousakis, K.A. Kirou, M.K. Crow, and J.G. Routsias. 2006. Elevated levels of soluble CD40 ligand (sCD40L) in serum of patients with systemic autoimmune diseases. *J. Autoimmun.* 26:165–171. http://dx.doi.org/10.1016/j.jaut.2006.02.002

Guiducci, C., R.L. Coffman, and F.J. Barrat. 2009. Signalling pathways leading to IFN-alpha production in human plasmacytoid dendritic cell and the possible use of agonists or antagonists of TLR7 and TLR9 in clinical indications. *J. Intern. Med.* 265:43–57. http://dx.doi.org/10.1111/j.1365-2796.2008.02050.x

Hao, Y., P. O'Neill, M.S. Naradikian, J.L. Scholz, and M.P. Cancro. 2011. A B-cell subset uniquely responsive to innate stimuli accumulates in aged mice. *Blood.* 118:1294–1304. http://dx.doi.org/10.1182/blood-2011-01-330530

Haywood, M.E., S.J. Rose, S. Horswell, M.J. Lees, G. Fu, M.J. Walport, and B.J. Morley. 2006. Overlapping BXSB congenic intervals, in combination with microarray gene expression, reveal novel lupus candidate genes. *Genes Immun.* 7:250–263. http://dx.doi.org/10.1038/sj.gene.6364294

Howe, H.S., K.O. Kong, B.Y. Thong, W.G. Law, F.L. Chia, T.Y. Lian, T.C. Lau, H.H. Chng, and B.P. Leung. 2012. Urine sVCAM-1 and sICAM-1 levels are elevated in lupus nephritis. *Int. J. Rheum Dis.* 15:13–16. http://dx.doi.org/10.1111/j.1756-185X.2012.01720.x

Ikeda, Y., T. Fujimoto, M. Ameno, H. Shiiki, and K. Dohi. 1998. Relationship between lupus nephritis activity and the serum level of soluble VCAM-1. *Lupus.* 7:347–354. http://dx.doi.org/10.1191/096120398678920172

Jego, G., A.K. Palucka, J.P. Blanck, C. Chalouni, V. Pascual, and J. Banchereau. 2003. Plasmacytoid dendritic cells induce plasma cell differentiation through type I interferon and interleukin 6. *Immunity.* 19:225–234. http://dx.doi.org/10.1016/S1074-7613(03)00208-5

Kato, K., E. Santana-Sahagún, L.Z. Rassenti, M.H. Weisman, N. Tamura, S. Kobayashi, H. Hashimoto, and T.J. Kipps. 1999. The soluble CD40 ligand sCD154 in systemic lupus erythematosus. *J. Clin. Invest.* 104:947–955. http://dx.doi.org/10.1172/JCI7014

Lande, R., J. Gregorio, V. Facchinetti, B. Chatterjee, Y.H. Wang, B. Homey, W. Cao, Y.H. Wang, B. Su, F.O. Nestle, et al. 2007. Plasmacytoid dendritic cells sense self-DNA coupled with antimicrobial peptide. *Nature.* 449:564–569. http://dx.doi.org/10.1038/nature06116

Lauwerys, B.R., and E.K. Wakeland. 2005. Genetics of lupus nephritis. *Lupus.* 14:2–12. http://dx.doi.org/10.1191/0961203305lu2052oa

Marshak-Rothstein, A., and I.R. Rifkin. 2007. Immunologically active autoantigens: the role of toll-like receptors in the development of chronic inflammatory disease. *Annu. Rev. Immunol.* 25:419–441. http://dx.doi.org/10.1146/annurev.immunol.22.012703.104514

Means, T.K., E. Latz, F. Hayashi, M.R. Murali, D.T. Golenbock, and A.D. Luster. 2005. Human lupus autoantibody-DNA complexes activate DCs through cooperation of CD32 and TLR9. *J. Clin. Invest.* 115:407–417. http://dx.doi.org/10.1172/JCI23025

Morel, L., K.R. Blenman, B.P. Croker, and E.K. Wakeland. 2001. The major murine systemic lupus erythematosus susceptibility locus, Sle1, is a cluster of functionally related genes. *Proc. Natl. Acad. Sci. USA.* 98:1787–1792. http://dx.doi.org/10.1073/pnas.98.4.1787

Nacionales, D.C., K.M. Kelly-Scumpia, P.Y. Lee, J.S. Weinstein, R. Lyons, E. Sobel, M. Satoh, and W.H. Reeves. 2007. Deficiency of the type I interferon receptor protects mice from experimental lupus. *Arthritis Rheum.* 56:3770–3783. http://dx.doi.org/10.1002/art.23023

Okamoto, A., K. Fujio, N.H. Tsuno, K. Takahashi, and K. Yamamoto. 2012. Kidney-infiltrating CD4+ T-cell clones promote nephritis in lupus-prone mice. *Kidney Int.* 82:969–979. http://dx.doi.org/10.1038/ki.2012.242

Pisitkun, P., J.A. Deane, M.J. Difilippantonio, T. Tarasenko, A.B. Satterthwaite, and S. Bolland. 2006. Autoreactive B cell responses to RNA-related antigens due to TLR7 gene duplication. *Science.* 312:1669–1672. http://dx.doi.org/10.1126/science.1124978

Rubtsov, A.V., K. Rubtsova, A. Fischer, R.T. Meehan, J.Z. Gillis, J.W. Kappler, and P. Marrack. 2011. Toll-like receptor 7 (TLR7)-driven accumulation of a novel CD11c+ B-cell population is important for the development of autoimmunity. *Blood*. 118:1305–1315. http://dx.doi.org/10.1182/blood-2011-01-331462

Santer, D.M., T. Yoshio, S. Minota, T. Möller, and K.B. Elkon. 2009. Potent induction of IFN-alpha and chemokines by autoantibodies in the cerebrospinal fluid of patients with neuropsychiatric lupus. *J. Immunol*. 182:1192–1201. http://dx.doi.org/10.4049/jimmunol.182.2.1192

Santer, D.M., A.E. Wiedeman, T.H. Teal, P. Ghosh, and K.B. Elkon. 2012. Plasmacytoid dendritic cells and C1q differentially regulate inflammatory gene induction by lupus immune complexes. *J. Immunol*. 188:902–915. http://dx.doi.org/10.4049/jimmunol.1102797

Santiago-Raber, M.L., R. Baccala, K.M. Haraldsson, D. Choubey, T.A. Stewart, D.H. Kono, and A.N. Theofilopoulos. 2003. Type-I interferon receptor deficiency reduces lupus-like disease in NZB mice. *J. Exp. Med*. 197:777–788. http://dx.doi.org/10.1084/jem.20021996

Shlomchik, M.J. 2009. Activating systemic autoimmunity: B's, T's, and tolls. *Curr. Opin. Immunol*. 21:626–633. http://dx.doi.org/10.1016/j.coi.2009.08.005

Spronk, P.E., H. Bootsma, M.G. Huitema, P.C. Limburg, and C.G. Kallenberg. 1994. Levels of soluble VCAM-1, soluble ICAM-1, and soluble E-selectin during disease exacerbations in patients with systemic lupus erythematosus (SLE); a long term prospective study. *Clin. Exp. Immunol*. 97:439–444. http://dx.doi.org/10.1111/j.1365-2249.1994.tb06107.x

Subramanian, S., K. Tus, Q.Z. Li, A. Wang, X.H. Tian, J. Zhou, C. Liang, G. Bartov, L.D. McDaniel, X.J. Zhou, et al. 2006. A Tlr7 translocation accelerates systemic autoimmunity in murine lupus. *Proc. Natl. Acad. Sci. USA*. 103:9970–9975. http://dx.doi.org/10.1073/pnas.0603912103

Swiecki, M., S. Gilfillan, W. Vermi, Y. Wang, and M. Colonna. 2010. Plasmacytoid dendritic cell ablation impacts early interferon responses and antiviral NK and CD8(+) T cell accrual. *Immunity*. 33:955–966. http://dx.doi.org/10.1016/j.immuni.2010.11.020

Teichmann, L.L., M.L. Ols, M. Kashgarian, B. Reizis, D.H. Kaplan, and M.J. Shlomchik. 2010. Dendritic cells in lupus are not required for activation of T and B cells but promote their expansion, resulting in tissue damage. *Immunity*. 33:967–978. http://dx.doi.org/10.1016/j.immuni.2010.11.025

Telles, R.W., G.A. Ferreira, N.P. da Silva, and E.I. Sato. 2010. Increased plasma myeloperoxidase levels in systemic lupus erythematosus. *Rheumatol. Int*. 30:779–784. http://dx.doi.org/10.1007/s00296-009-1067-4

Theofilopoulos, A.N., R. Gonzalez-Quintial, B.R. Lawson, Y.T. Koh, M.E. Stern, D.H. Kono, B. Beutler, and R. Baccala. 2010. Sensors of the innate immune system: their link to rheumatic diseases. *Nat. Rev. Rheumatol*. 6:146–156. http://dx.doi.org/10.1038/nrrheum.2009.278

Tian, J., A.M. Avalos, S.Y. Mao, B. Chen, K. Senthil, H. Wu, P. Parroche, S. Drabic, D. Golenbock, C. Sirois, et al. 2007. Toll-like receptor 9-dependent activation by DNA-containing immune complexes is mediated by HMGB1 and RAGE. *Nat. Immunol*. 8:487–496. http://dx.doi.org/10.1038/ni1457

Vakkalanka, R.K., C. Woo, K.A. Kirou, M. Koshy, D. Berger, and M.K. Crow. 1999. Elevated levels and functional capacity of soluble CD40 ligand in systemic lupus erythematosus sera. *Arthritis Rheum*. 42:871–881. http://dx.doi.org/10.1002/1529-0131(199905)42:5<871::AID-ANR5>3.0.CO;2-J

Vilá, L.M., M.J. Molina, A.M. Mayor, J.J. Cruz, E. Ríos-Olivares, and Z. Ríos. 2007. Association of serum MIP-1alpha, MIP-1beta, and RANTES with clinical manifestations, disease activity, and damage accrual in systemic lupus erythematosus. *Clin. Rheumatol*. 26:718–722. http://dx.doi.org/10.1007/s10067-006-0387-y

Vollmer, J., S. Tluk, C. Schmitz, S. Hamm, M. Jurk, A. Forsbach, S. Akira, K.M. Kelly, W.H. Reeves, S. Bauer, and A.M. Krieg. 2005. Immune stimulation mediated by autoantigen binding sites within small nuclear RNAs involves Toll-like receptors 7 and 8. *J. Exp. Med*. 202:1575–1585. http://dx.doi.org/10.1084/jem.20051696